NEW INSIGHTS INTO THE CRUSTAL STRUCTURE OF THE NORTH GERMAN BASIN FROM REPROCESSING OF SEISMIC REFLECTION DATA

M. Yoon, M. Baykulov, S. Dümmong, H.-J. Brink, and D. Gajewski

email: *mi-kyung.yoon@zmaw.de*

keywords: *Deep crustal images, reflection Moho, Glückstadt-Graben, Common Reflection Surface stack, North German Basin*

ABSTRACT

The influence of deep crustal processes on basin formation and evolution and its relation to current morphology is not yet well understood. A key feature to unravel these issues is a good seismic image of the crust. A part of the data recorded by the hydrocarbon industry in the late 1970ies and 1980ies in the North German Basin was released to the public recently. These observations were recorded up to 15 s TWT and have a mean fold of about 20 which is very low compared to current acquisitions. The processing so far was focused on the sedimentary structures due to the hydrocarbon potential of the area. A specialized contemporary processing like the Common Reflection Surface (CRS) stack technology which is particularly suited for low fold data shows a considerably improved imaging quality compared to the Common Midpoint (CMP) processing performed in the 1980ies. This applies not only to lower crustal features but also holds for the images of the sedimentary structure and the salt plugs. The reprocessed images display an almost flat Moho discontinuity even in the area of the Glückstadt-Graben where a lower crustal high density body was discovered.

INTRODUCTION

The North German Basin is part of the Central European Basin system CEBS. It is a multiphase basin with extensive salt tectonics (Maystrenko et al., 2005). The Glückstadt Graben is a local feature in the North German Basin. It was affected by strong salt tectonics during the late Triassic and Cretaceous. As one of the deepest post-Permian Graben structures it provides a structural record of stress and strain states imprinted into the crustal and mantle structure. The basin structure and the sedimentary fill of the Graben were widely investigated during the last decades (Bachmann and Grosse, 1989; Brink et al., 1990, 1992; Brink, 2003; Baldschuhn et al., 2001; Kockel, 2002; Maystrenko et al., 2005; Scheck-Wenderoth and Lamarche, 2005). Due to the oil and gas exploration potential an extensive seismic reflection database was gathered in the North German Basin and the area of the Glückstadt Graben by the industry in the early 1980ies. The acquisition layout and the processing parameters were tuned to image the basin sediments down to the Zechstein only (ca. 3 s TWT). The imaging was performed using standard CMP processing which was state of the art in the 80ies. This processing yielded detailed images of the shallow part in the poststack time sections and provided the basis for extensive seismic stratigraphic interpretations (Maystrenko et al., 2005). But the potential of the data to image the subsedimentary part such as the crystalline crust was never optimized and only marginally exploited. Also, the imaging results within and in the vicinity of the salt plugs were rather poor.

Essential parts of this data base became available for research within the SPP 1135 Dynamics of Sedimentary Systems. One aim of the SPP was to study the influence of deep rooted processes on formation and evolution of the North German Basin and their relation to neo-tectonic activities. Also, Moho depth,

Moho relief, Moho diversity and possible metamorphic complexes and their effects on seismic signatures are some of the key issues to be investigated to understand the basin evolution. Moreover, seismic events within the crystalline crust as well as fault zones and their possible surface extensions are further topics to be studied.

In order to extract additional information that might provide important information on deep processes steering and influencing basin formation we reprocessed the data sets with the main focus on imaging structures in the lower crust. The reprocessing was performed using the Common Reflection Surface (CRS) stack method (Tygel et al., 1997; Müller, 1999; Mann, 2002). In contrast to the classical CMP stack procedure the CRS stack can be performed without an explicit knowledge of a macro velocity model. It also provides additional parameters that can be used for subsequent processes, e.g. velocity model building and multiple suppression (Zaske et al., 1999; Duveneck, 2004).
The CRS stack has already been successfully applied by the hydrocarbon industry for processing reflection data from sedimentary basins (Trappe et al., 2001). Also, first applications of the CRS stack method to crustal reflection data (4 s TWT) from the Donbas foldbelt in the Ukraine (Menyoli et al., 2004) showed that this technology is suitable for imaging in complex overthrust environments.

This paper presents the results which we obtained by reprocessing of seismic reflection data using the CRS stack method. The results will be presented in comparison with time sections obtained by classical CMP stack processing. In the following, first the CRS stack will be shortly introduced. In part 3 an introduction to the geological setting of the study area and the data base is given. The data processing and the new results are presented in part 4 and 5. A discussion of the new results and a conclusion finalize the paper.

THE COMMON REFLECTION SURFACE STACK METHOD

The Common Reflection Surface (CRS) stack technology for processing reflection seismic data was recently developed (Schleicher et al., 1993; Tygel et al., 1997; Müller, 1999; Mann, 2002) and is currently applied to data from sedimentary environments (Trappe et al., 2001; Bergeler et al., 2002) for hydrocarbon exploration. The CRS stack method is a multiparameter stacking method, where the parameters have several important applications for seismic imaging, tomography, stacking velocities, multiple removal and spreading corrections just to name a few (Duveneck, 2004; Zaske et al., 1999; Vieth, 2001; Hoecht, 2002). The application of this technology to low fold data is of particular importance since it leads to an improved signal to noise ratio by stacking more traces than the classical Common Midpoint (CMP) stack. In the CRS stack procedure the local dip of the structures is automatically acknowledged and does not require any particular dip move out (DMO) processing. Despite these facts, this technique has not yet been applied to deep crustal reflection seismic data.

The seismic reflection data recorded by the hydrocarbon industry in the late 1970ies and 1980ies were recently released to the public. These data were recorded up to 15 s, have a low fold of about 20 and were CMP processed in the 1980ies. No tuned processing to optimize the images of the lower crust was applied. The CRS stack technology appears to be very well suited to perform an optimized imaging of features within the crystalline rocks of the lower crust. This processing and its results are discussed in the following sections.

GEOLOGICAL SETTING AND THE DATA SETS

Study area and geology

The study area is located in the North German Basin, a part of the Central European Basin system CEBS (Figure 1). A number of deep seismic experiments were carried out to investigate the crustal and mantle structure throughout the CEBS (Trappe, 1989; Reichert, J.C., 1993; Abramovitz et al., 1998; DEKORP-BASIN Research Group, 1999; Maystrenko et al., 2003). Thereby, the area of the Glückstadt Graben was of special interest in order to reveal the deep crustal structures along the transition zone from the Precambrian Fenno-Scandian Shield to the Caledonian crust in NW Germany. The Glückstadt Graben is located right between the North Sea in the west, the Baltic Sea in the east and between the Rynkoebing-Fyn High in the north and the Elbe-Odra Line (EOL, Figure 1) in the south. It is one of the deepest Mezozoic graben structures within the CEBS providing the stress and strain history of this area inherited

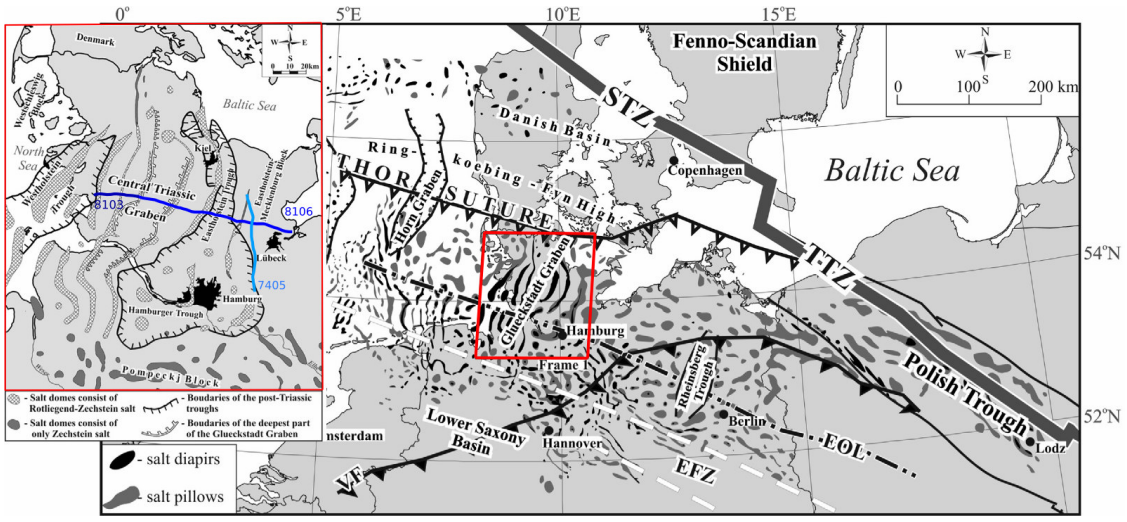

Figure 1: Location of the study area with the major structural units of the Central European Basin (modified after Maystrenko et al. (2005)). STZ: Sorgenfrei-Tornquist Zone, TTZ: Teisseyre-Tornquist Zone, EOL: Elbe-Odra Line, EFZ: Elbe Fault Zone, VF: Variscan Front. Box: Overview of the seismic reflection profiles. Line 8106, its western extension line 8401, and line 7405 are located north of the Elbe lineament.

in its crustal and deeper structure. During the Middle-Late Triassic (Keuper) the Glückstadt Graben was affected by extension where rapid subsidence took place within the central part of the Graben accompanied by strong salt tectonics (Maystrenko et al., 2005). Relative uplift with regional erosion of the elevated relief took place in the late Jurassic to early Cretaceous. Another pulse of salt movements occurred which was correlated with an extensional event in the Pompeckj Block and the Lower Saxony Basin. During the Cenozoic subsidence along the marginal parts of the Graben was reactivated and accelerated by the development of a strong subsidence center in the North Sea.

The data sets

To further study the detailed crustal structure using new processing technology which is especially suited for data with low coverage three seismic reflection lines were reprocessed: the north-south heading line 7405 and the east-west heading line 8106, and its western extension line 8401. All profiles are located north of the Elbe lineament (EOL, Figure 1). Line 7405 is located to the east of the Glückstadt Graben and runs parallel to the Graben axis. Line 8106 and line 8401 were aligned perpendicular to the Graben axis and are crossing the Graben over its whole east-west extension.

The acquisition parameters of the data sets were different. The north-south heading profile line 7405 is 65 km long and comprising 590 shot gathers (see also Table 1). Each of the shot gathers consisted of 48 receivers with 100 m spacing. The shot spacing was also about 100 m. The sampling rate is 4 ms and the total recording length 15 s. This acquisition leads to 1321 CMPs with a CMP spacing of 50 m for this profile. The maximum CMP fold of line 7405 is only 25. The mean CMP fold is between 15 and 20.
Line 8106 represents the largest data set of the considered profiles. It consists of 771 shot gathers. The shot point spacing is 120 m. Each shot was recorded using 120 receivers with a spacing of 40 m. The resulting maximum offset is 4800 m. The sampling rate during recording was 2 ms, the total recording time 13 s. The resulting 4649 CMPs lead to a total profile length of ca. 92 km and a mean CMP fold of about 20.
Line 8401 was recorded as the western extension of line 8106. It comprises 553 shot gathers. The acquisition parameters were similar to the parameters of line 8106 (120 geophones per shot, 40 m receiver spacing, 13 s recording time). Due to the irregular shot spacing an irregular acquisition pattern is obtained. The CMP fold varies between a minimum of about 15 and a maximum of 58. The mean CMP fold is 30. This acquisition results in 1725 CMP gathers with a midpoint spacing of 20 m. The total profile length was ca. 35 km. For line 8106 stacking velocities as obtained from processing the data in the 1980ies were

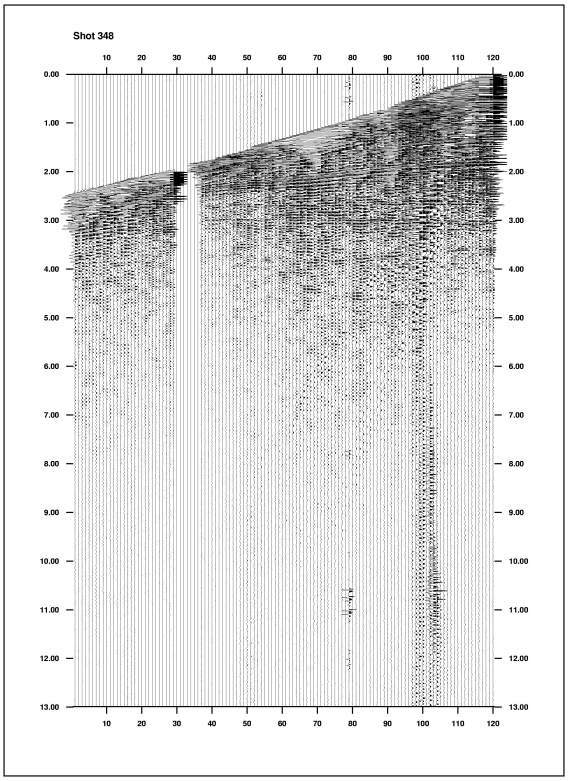

Figure 2: Data example. A shot gather from line 8106. The signal to noise ratio of the data is rather low with strong first arrivals of the direct and the refracted waves. However, strong reflections from the Zechstein base are already visible at about 3 s TWT.

provided as printed paper copies.

	Line 7405	Line 8106	Line 8401
Number of shots	590	771	553
Shot point spacing [m]	100	120	120
Receiver spacing [m]	100	40	40
Receivers per shot	48	120	120
Maximum offset [m]	4800	4800	4800
CMP interval [m]	50	20	20
CMP-coverage	~ 20	~ 20	~ 30
CMP locations	1320	4649	1725
Line length [km]	~ 65	~ 92	~ 35
Sampling interval [ms]	4	2	2
Total recording time [s]	15	13	13

Table 1: Acquisition parameters of line 8106, line 8401 and line 7405. Note the low fold of the data compared to contemporary acquisitions.

A typical example of a shot gather before preprocessing is shown in Figure 2. Besides the strong first arrivals of the direct and the refracted wave strong reflections from the base of the Zechstein are already visible in the raw data at about 3 s TWT. Deep reflection events are hardly visible, whereas dead and noisy traces are present at several locations. In general, the signal to noise ratio of the shot gathers was comparably low.

Data processing

The processing of the data was split into two major parts. In the first part the data were processed using the classical CMP processing flow similar to the flow used in the 1980ies. The resulting CMP stack sections were compared to the available industry paper sections. This was done in order to achieve a comparable processing level for better determination of later improvements in the reprocessing. In the second part the data sets were processed using the CRS stack method.

Prior to the CMP and CRS stack the data were preprocessed to enhance the data quality. The preprocessing is a prerequisite to obtain reasonable seismic images. It is particularly important for low fold data with poor signal to noise ratio. The preprocessing sequence applied to the data started with the application of the proper geometry on the data sets. After static corrections and residual static removal the shot gathers were trace edited. This included the removal of bad traces, elimination of noise e.g. high-frequency spikes. Furthermore, top muting was applied to remove first arrivals of direct and refracted waves. Also, bottom mute was applied to eliminate systematic incoherent noise, e.g. instrument noise on all traces at later arrival times. The maximum frequencies of the data sets were up to 90 Hz high. The central frequencies were around 30 Hz. Finally, the data sets were filtered using a bandpass filter of 5 - 50 Hz.

CMP stack

In order to compare recent results obtained by the application of contemporary processing techniques to images from conventional methods, the data sets were imaged using the classical CMP stack procedure. A stacking velocity model as obtained by former processing was only available for line 8106. This model was used to compute the CMP stack sections for line 8106. For line 8401 a velocity analysis was performed at selected CMP locations. Automatic linear interpolation provided the stacking velocity model. After the stack an automatic gain control was applied to the sections. Furthermore the stacked sections of 8401 and 8106 were merged together to form an extended east-west heading line such that line 8401 was pasted to line 8106 at CMP location 4600 of line 8106.

For line 7405 no velocity information was available and conventional velocity analysis could not be performed due to the low signal to noise ratio. To compute a CMP stack section the stacking velocity information along line 8106 was manually edited and adjusted to line 7405. The stacking velocity model was build at sparse CMP positions and iteratively upgraded by analyzing the image quality of the resulting CMP stack sections. A linear automatic interpolation of the velocity field between the CMP locations yielded the stacking velocity model used to compute the final CMP stack section shown in Figure 3. South (CMP 1) is located left and north (CMP 1320) to the right.

For line 8106 the stacking velocity model from former processing was available. In some parts of the profile additional stacking velocity analyses at a few CMP locations were added for better resolution of velocities and improved imaging. The CMP stack sections of line 8106 and line 8401 were computed separately. An automatic gain control was applied to the CMP stack sections. Afterwards, the stacked sections were merged together at CMP position 4600 of line 8106 (Figure 5). The CMP location numbers of line 8106 were continued for line 8401 towards the west. This resulted in ca. 6000 CMP locations along the combined section. The section is running from east (CMP 1, right) to west (CMP 6000, left).

CRS stack

The CRS stack was applied to the preprocessed data that were resorted into CMP gathers. In order to enhance the reflection amplitudes at deeper levels an automatic gain control (AGC) was additionally applied to the data prior to the CRS stack. The time window of the AGC was 1000 ms. The CRS stack sections were computed for each data set for 3 different CRS stack parameter sets to determine the optimum stacking apertures. The most crucial part was to adjust the time dependent stacking apertures such that both near subsurface structures as well as lower crustal structures are imaged properly. The size of the stacking aperture was in the range of the first Fresnel zone for a given centre frequency of the wavefield at the targeted image depth. The CRS stack sections of line 7405 and line 8106-8401 are shown in Figure 4 and Figure 6, respectively. A detailed discussion of the results will be given in the following chapter.

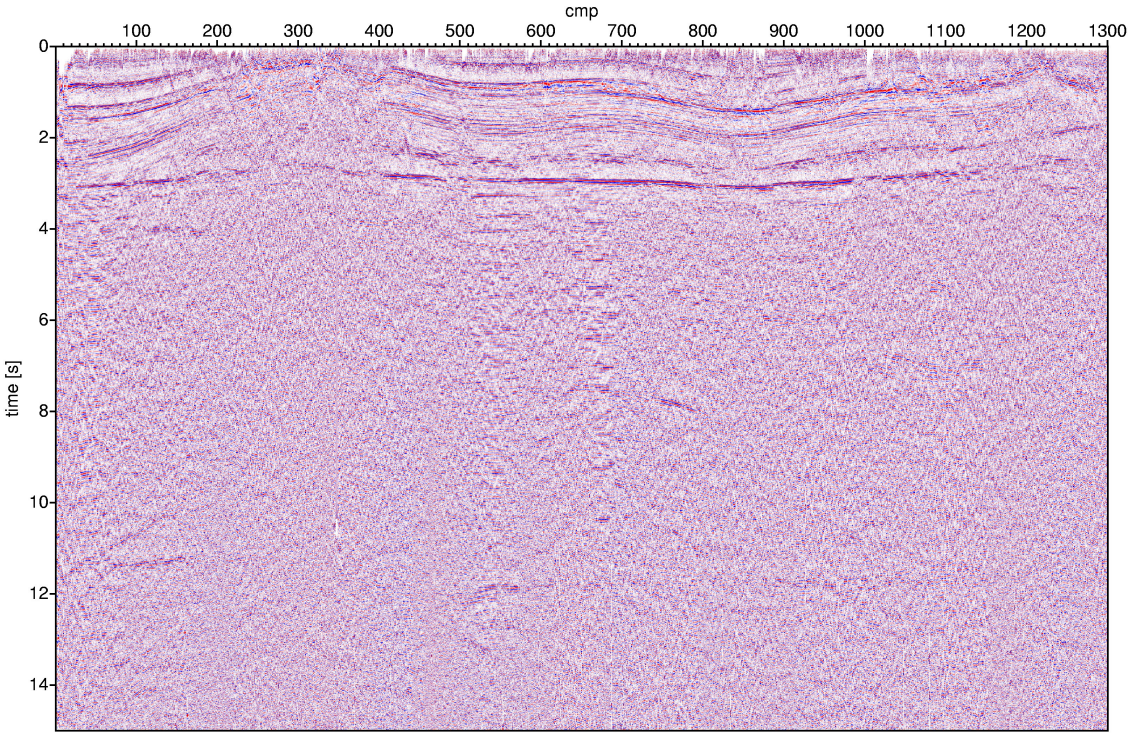

Figure 3: CMP stack of line 7405. The sedimentary part down to 3 s TWT shows several events, whereas reflections in the deeper crustal part are hardly identified.

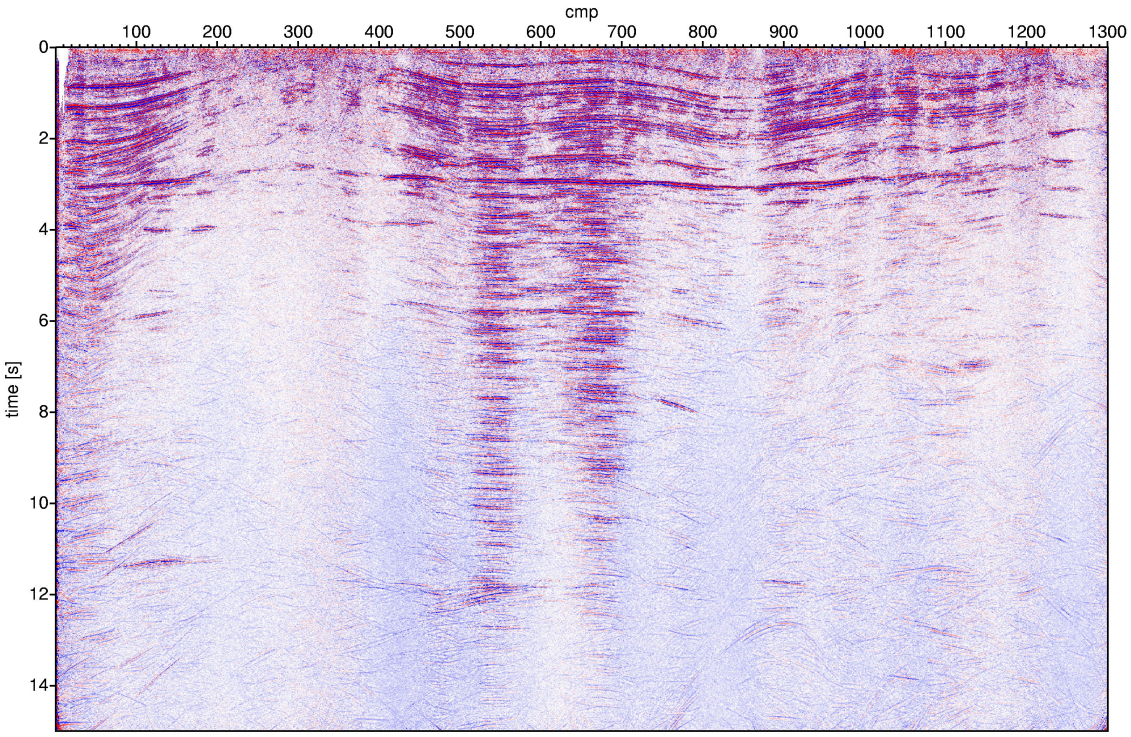

Figure 4: CRS stack of line 7405. The image of the sedimentary layers is enhanced, including few multiple events. However, the image of crustal reflections are improved with respect to their visibility and continuity. Furthermore, deep reflections at 11.5-12 s TWT, referred to as reflections from the Moho, are identified.

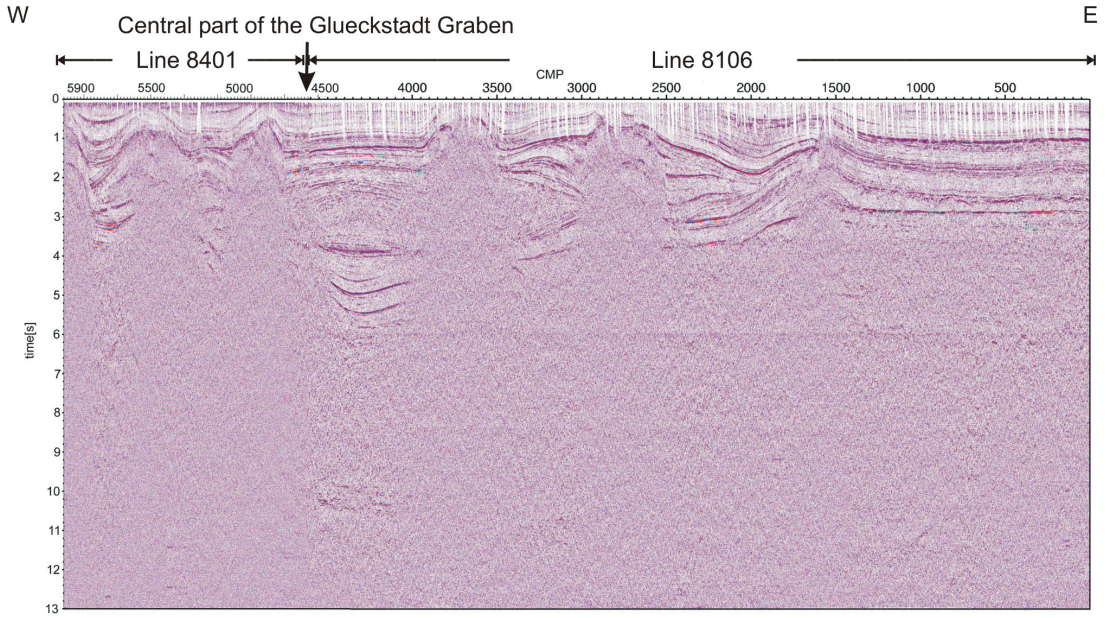

Figure 5: CMP stack section of line 8106-8401. The sedimentary cover is well imaged whereas deeper crustal reflections are hardly visible.

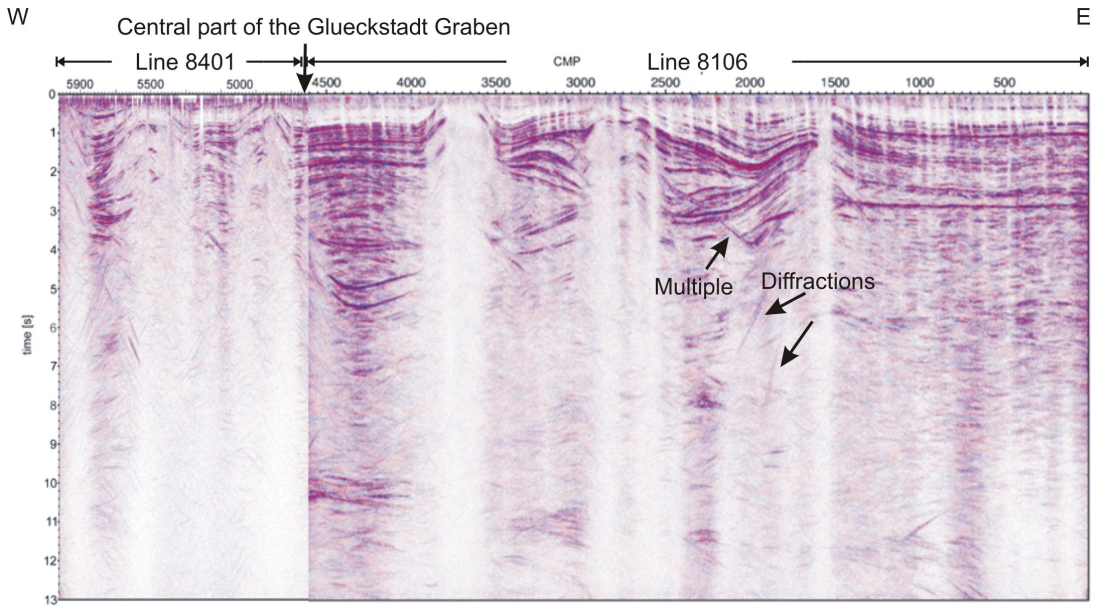

Figure 6: Merged CRS stack sections of line 8106 and line 8401 (The vertical arrow marks the intersection of the two profile at CMP 4600 in line 8106. The CMP locations are counted up for the CMP locations of line 8401 towards the west. Note that the amplitude level changes due to different acquisition parameters). The CRS stack section shows an enhanced image of reflections at all depth levels, but also coherent energy e.g. multiples and diffractions are enhanced. The images of the internal salt structures as well as crustal and Moho reflections (between 10-11 s) are significantly enhanced. The CRS stack section also indicates higher crustal reflectivity in the western part of the profile than in the eastern part. This might indicate different tectonic stages of the crustal units east of the Glueckstadt Graben and in the central part of it. The crustal image appears almost transparent below the salt plugs and below the steep fault at CMP 1500-1600 because the latter leads to the loss of coherent energy, thus no reflections were imaged during the CRS stack.

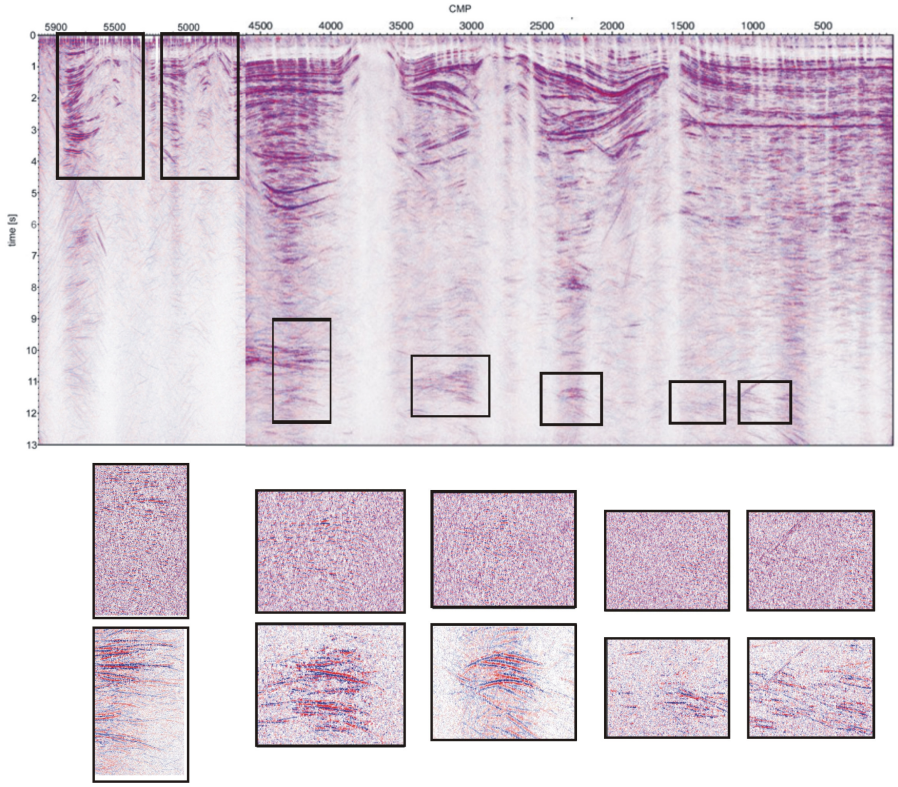

Figure 7: Comparison of reflections from the deeper crust in the CMP and in the CRS stack section. Comparison of the zoomed internal salt reflections (rectangles between CMP 4700-5200 and CMP 5300-5900) are shown in Figure 8.

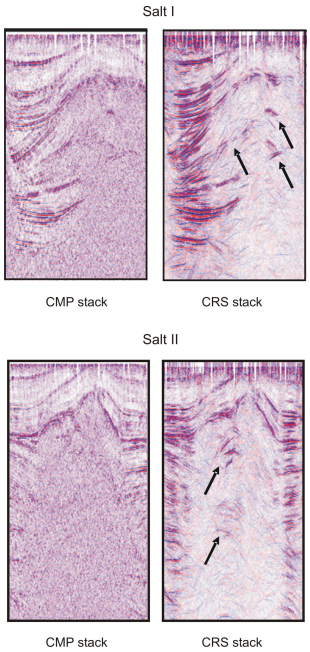

Figure 8: The comparison of the CMP (left) and the CRS stack (right) shows that the CRS stack significantly enhanced the visibility of internal salt reflections. In both salt plugs reflections revealing the internal structure can be clearly identified and traced (see arrows).

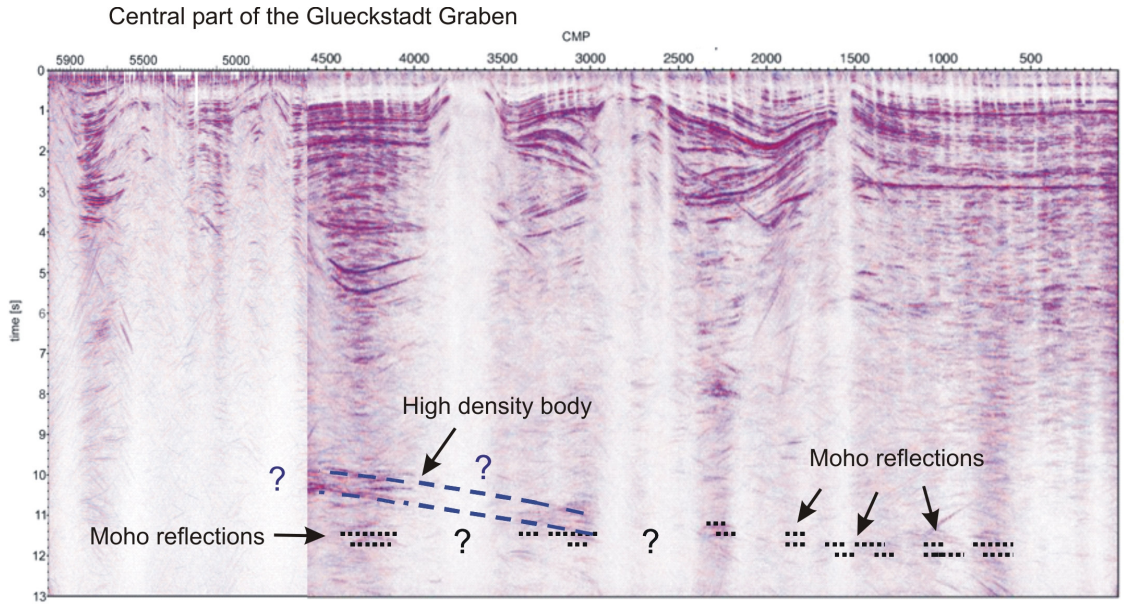

Figure 9: Interpretation of the deep crustal reflections observed in line 8106-8401. With respect to their reflection strength and their continuity the horizontal weak and more discontinuous reflections at ca. 11.5 s TWT are interpreted as reflections from the Moho (black dashed), implicating a flat Moho topography along the Glueckstadt Graben. The stronger east dipping reflections below the central part of the Graben are associated with the existence of a wedge-shaped lower crustal body with a relatively high impedance contrast. The latter interpretation is in good agreement with recent results from gravity modeling in this area (Yegerova et al., 2006).

RESULTS AND DISCUSSION

As described in the previous chapter the reprocessing yielded two seismic sections: The 65 km long south-north heading profile 7405 and the combined east-west ca. 120 km long profile 8106-8401 crossing the Glückstadt Graben.

Line 7405

Figure 3 shows the CMP stack section of line 7405. The sedimentary fill down to about 2 s TWT and the prominent reflections from the Zechstein base at 3 s TWT are clearly and almost continuously imaged throughout the whole profile. In the southern part of the profile between CMP 150 and 400 a salt body is visible between 0 - 3 s TWT. Within the salt body reflections are only poorly imaged. Below the Zechstein reflector the section hardly reveal clear reflections. Coherent reflections are hardly visible in the deeper parts of the section. Only some weak events in the lower crust can be identified between CMP 90 and 150, and CMP 500 and 600 at 11.5 s TWT and 12 s TWT, respectively.
The CRS stack section of line 7405 (Figure 4) shows an improved signal to noise ratio, especially within the salt body (CMP 150 - 400) and within the crust. The reflections from the sedimentary part appear stronger and more pronounced compared to the corresponding reflections in the CMP stack section. However, multiples are also enhanced in the CRS stack section, especially in the area of the salt flanks at 0 - 3 s TWT between CMP 1 and 150, and CMP 450 and 500 and in the middle of the profile between CMP 500 and 700. There, very strong internal multiples from the sediments and a strong multiple from the Zechstein base (e.g. ca. 6 s TWT) dominate the image down to ca. 11 s TWT.
The image of the salt structure reveals reflections within the salt body between 1 - 2.5 s TWT. Also, the reflection from the Zechstein base at 3 s is imaged almost continuously throughout the salt plug. Below the salt plug at ca. 4 s TWT, almost horizontal crustal reflections are visible that were only hardly identified in the CMP section (between CMP 100 and 200 and between CMP 350 and 480).

The upper and the lower crust appear almost transparent in the southern part of the profile (CMP 150 - 450). This is due to the salt body located above causing strong scattering of the wavefield and thus distortion of coherent energy leading to an apparently transparent image. These areas appear much more transparent in the CRS stack than in the CMP stack. This is due to the fact, that the CRS method uses much more traces for the stack compared to the CMP stack processing. Therefore the signal to noise ratio is increased and incoherent noise is removed which is strongly affecting the CMP image. In the northern part of the profile (between CMP 750 and 1300) the crust appears weakly reflective revealing only some short reflections in the upper crust between 3 - 8 s TWT. In the deeper part of the section horizontal reflections are visible in the southern part of the section (CMP 90 - 150) at 11.5 s TWT and in the middle (CMP 500 - 560) and in the northern part (CMP 890 - 930) at 12 s TWT. These reflections are interpreted as Moho reflections, indicating an almost flat Moho topography in north-south direction toward the Elbe-Odra-Line. The Moho reflections in the southern part (CMP 90 - 150) of the profile appear more pronounced than the reflections in the middle (CMP 500 - 560) and in the northern part (CMP 890 - 930), which are narrow in time and weak in amplitude. Also, some steep dipping events in the lower crust are visible which are associated with diffraction events.

Line 8106-8104

In the following the combined lines 8106 and 8401 are referred to as line 8106-8401. Figure 5 displays the CMP stack section of line 8106-8401. The CMP section provides a very detailed image of the sedimentary part down to the Zechstein base at 3 s TWT as well as of the salt plugs between CMP 2500 and 3000, CMP 3500 and 4000, CMP 4750 and 5200, and CMP 5300 and 5800. At CMP 1500 a steep fault is clearly visible, which separates the Eastholstein Trough in the west from the Eastholstein-Mecklenburg block in the east (Maystrenko et al., 2005). Also, sharp parallel dipping reflections are observed in the upper crust between 4 and 5 s TWT (CMP 4000 - 4500) that can be correlated with two parallel dipping reflections between CMP 3000 and 3500 at 3 to 4 s TWT. In the deeper parts reflections are hardly identified.

Figure 6 shows the CRS stack of line 8106-8401. The lateral abrupt change in reflection amplitude at CMP 4600 marks the location where line 8106 and line 8401 were merged together (marked by the vertical arrow). Lateral amplitude balancing was not applied to the merged stack. The differences in amplitudes and signal to noise ratio are due to the different acquisition parameters of the two lines. The comparison of the CMP stack section with the CRS stack section shows that the CRS stack significantly improved the signal to noise ratio and generally improved the image quality, especially in the deeper parts of the sections. The image of the sedimentary cover as well as of internal salt structures is clearer and more detailed than in the CMP stack section.

However, strikingly the CRS stack section appears laterally separated into reflective and less reflective crustal parts. This is due to the salt plugs in the near surface (see CMP 2500 - 3000, CMP 3500 - 4000, CMP 4750 - 5200, and CMP 5300 - 5800) which - as highly heterogeneous structures - cause strong scattering and thus the loss of coherency of deeper reflections. Loss in coherency in the upper part of the section directly influences the CRS stack image of the deeper parts below as subsequently no coherent energy can be stacked. This holds as well for the lack of deeper reflections between CMP 1500 and 1600, where the image is distorted due to a steep surface reaching fault. Besides, all coherent energy contained in the data is enhanced by the CRS stack. This includes diffraction events as well as multiple arrivals (see Figure 6) if the final stack is not performed to suppress these events. Reflection events in the lower crust are enhanced by the CRS stack and better visible compared to the CMP stack section. For example a mid crustal reflection between CMP 2200 and 2350 at about 8 s TWT can be clearly identified (Figure 6) which was only hardly visible in the corresponding CMP stack section (Figure 5). Also, between CMP 1 and CMP 1500 the reflections in the upper crust are significantly enhanced. The CRS stack section reveals apparently different reflectivity in the eastern part of the profile and below the Glückstadt Graben in the middle part of the profile. In the eastern part the upper crust appears more reflective, revealing a ca. 5 - 6 s long band of horizontal reflections. In the central part of the profile the reflectors in the upper and lower crust are comparably weak. Crustal reflections appear to be strongly diminished in the western part (line 8401). However, a direct comparison of reflection amplitudes observed for line 8601 and line 8401 is not possible since no amplitude preserving processing was applied and different acquisition parameters affect the reflection amplitudes in the stacked sections. Additionally, the image of the crustal part is presumably

affected by the salt bodies above, similar to the areas in line 8106 below the salt plugs (CMP 2500 - 3000, and CMP 3500 - 4000).
In the deeper part of the section below 10 s crustal reflections are enhanced in the CRS stack (see also Figure 7). Very prominent parallel east dipping continuous reflections are visible in the central part of the sections at ca. 10 - 11 s TWT between CMP 3800 and 4800. Further to the east the reflections are weaker and less continuous. Below the strong east dipping reflections between CMP 4000 and 4600 horizontal weak reflections can be identified.
Besides the enhancement of crustal and Moho reflections which was the major target of the reprocessing the CRS stack also improved the images of the salt plugs. A direct comparison of the imaged salt structures shows that the reprocessed results display details of the salt interior not seen before (Figure 8). These reflections may be interpreted as Keuper salt horizons which would point to a different internal structure of the salt plugs than previously thought of and currently applied (Maystrenko et al., 2005). This observation, however, needs further confirmation by additional processing, particularly prestack depth migration after careful velocity analysis. Such processing would image the salt area with a technology not yet applied to this data. In areas of great geological complexity and strong lateral velocity variations like salt structures prestack depth migration should be superior to the CMP and CRS stack. However, in order to obtain a qualitatively high prestack depth image an appropriate velocity model is required.

Mid crustal reflections

The CRS stack section of the profile 8106-8401 shows apparently different reflectivity patterns in the eastern part than in the western part. In the eastern part the section reveals a comparably highly reflective upper crust within a 3 to 4 s wide band. This area was tectonically less active than the area in the western part of the profile where less reflectivity is observed. Also, a pronounced reflection band is visible at about 6 s TWT between CMP 1 and 1000. These reflections are attributed to the Conrad discontinuity which is commonly observed at depths between 10 and 25 km (Chen, C.C. and Chen, C.S., 2000; Snelson et al., 2002). Between CMP 4000 and 4500 two sharp parallel reflectors are visible between 5.5 - 6.5 s TWT. These reflections correlate with a high conductivity body observed in magnetotelluric data (Hengesbach, 2006). This high conductivity body is attributed to a bitumen and pyrite rich blackschist body which indicates that the Glückstadt Graben has been developed as a pre-Triassic structure.

Moho reflections

The Moho below the Glückstadt Graben was interpreted to increase by about 4 km below the graben proper (Bachmann and Grosse, 1989; Brink et al., 1990) forming a pronounced bump in its topography. The reflections corresponding to this interpretation are clearly visible as the strongest events at deeper parts of the crust below the graben at about 10 s TWT (Figure 9). However, a careful inspection of the reflections with respect to their amplitudes and continuity revealed that these reflections are different from all other Moho reflections in this section (see, e.g., Moho events at CMPs 3200, 2300 and 600-1800 at about 11 - 11.5 s TWT, magnified excerpts of these parts of the data are displayed in Figure 7). The east dipping reflections observed in the central part of the Glückstadt Graben at about 10 - 11 s TWT are much stronger in amplitude and appear more continuous compared to the other events interpreted as Moho reflections in this section. Moreover, the weaker horizontal reflections at 11.5 s TWT exactly correspond in character to the events interpreted as Moho reflections elsewhere for this line. Therefore, we interpret the stronger east dipping reflections not as Moho reflections, but as lower crustal events. We further associate these east dipping reflections as reflections from a wedge-shaped lower crustal body with a relatively high impedance contrast. Consequently this interpretation proposes a flat Moho topography at about 11.5 s TWT throughout the section which only slightly increases at the far eastern part of the section. The proposed flat Moho is in conflict with the currently supported extension model of the Glückstadt Graben requiring a Moho high below the Glückstadt Graben. A flat Moho topography would be in good agreement with the observations of the DEKORP and DOBRE profiles where also a flat Moho is observed for the North German Basin and the Dnjepr-Donetz Basin, respectively (Bayer et al., 1999; Hoffmann and Brink, 2001). The proposed lower crustal body with a high impedance contrast below the Glückstadt Graben is in good agreement with recent gravity modeling results for this area (Yegerova et al., 2006).

SUMMARY AND CONCLUSIONS

We reprocessed reflection seismic data released by the hydrocarbon industry with the special emphasize to improve the image of the lower crust in order to investigate the influence of old deep rooted processes to the evolution of the CEBS. The reprocessing of seismic reflection lines to the north of the Elbe lineament was performed using the CRS stack method. The comparison of the CRS stack section with the results from conventional CMP stack processing showed that the reprocessing yielded improved image quality for all three processed reflection lines. The images provided new insights for the sedimentary cover of the basin and for the deeper parts of the crust in the area of the Glückstadt Graben. The following results are the key observations for the reprocessed sections:

- improved images of primary reflections at all crustal levels,
- improved resolution of the internal structure of salt plugs along the Glückstadt Graben indicating the presence of Keuper salt,
- several short horizontal reflections at mid crustal level not identified before,
- significant enhancement of deep crustal reflections,
- varying lower and mid crustal reflectivity patterns along the Glückstadt Graben profile,
- observation of a flat Moho throughout the North German Basin and the area below the Glückstadt Graben and the presence of a high density lower crustal body.

The latter points contradict the existing models of graben formation and therefore need further investigation and an extension of the database to the south of the Elbe lineament for better correlation with known crustal blocks. Different reflectivity patterns for the middle and lower crust were found where a correlation with respect to tectonic activity of the respective area seems to be apparent. This qualitative observation, however, needs further inspection since a quantitative amplitude discussion is difficult since the data were acquired with different parameters and true amplitude processing was not performed. The presented and discussed results clearly show the advantages of CRS stack processing for crustal data compared to classical CMP processing. However, as the CRS stack enhances all coherent energy contained in the data multiples and diffraction events might appear dominant in some parts of the stacked sections if the CRS stack parameters in the final stack are not specially adjusted to suppress them. This needs further processing and poststack migration. Nevertheless, particularly for data with low fold the CRS stack technology is clearly superior compared to the processing flow used in the 1980ies. This data example shows that the CRS stack method is a meaningful imaging technique for crustal reflection data sets.

ACKNOWLEDGMENTS

We thank the German Society for Petroleum and Coal Science and Technology (DGMK) for kindly providing the seismic data sets and supplemental material. The authors are also grateful for funding by the German Research Foundation (DFG, grant Ga 350/12-1) of the SPP 1135 – *Dynamics of Sedimentary Systems under Varying Stress Conditions: The Example of the Central European Basin-System* and the Wave Inversion Technology (WIT) consortium for providing the CRS stack code.

REFERENCES

Abramovitz, T., Thybo, H., and MONA LISA Working Group (1998). Seismic structure across the Caledonian Deformation Front along MONA LISA 1 profile in the southeastern North Sea. *Tectonophysics*, 288:153–176.

Bachmann, G. H. and Grosse, S. (1989). Struktur und Entstehung des Norddeutschen Beckens - geologische und geophysikalische Interpretation einer verbesserten Bouguer-Schwerekarte. *Nds. Akad. Geowiss. Veröfftl.*, 2:23–47.

Baldschuhn, R., Binot, F., Fleig, S., and Kockel, F. (2001). Geotektonischer Atlas von Nordwest Deutschland und dem deutschen Nordsee-Sektor. *Geologisches Jahrbuch*, A(153):3–95.

Bayer, U., Scheck, M., Rabbel, W., Krawczyk, C., Götze, H., Stiller, M., Beilecke, T., Marotta, A.-M., Barrio-Alvers, L., and Kuder, J. (1999). An integrated study of the NE-German Basin. *Tectonophysics*, 314:285–307.

Bergeler, S., Hubral, P., Marchetti, P., Cristini, A., and Cardone, G. (2002). 3D common-reflection-surface stack and kinematic wavefield attributes. *The Leading Edge*, 21(10):1010–1015.

Brink, H.-J. (2003). Die Entstehung des Norddeutschen Beckens - ein Metamorphosemodell. *DGMK-Tagungsbericht 2003-1*, pages 151–175. ISBN 3-936418-03-9.

Brink, H.-J., Dürschner, H., and Trappe, H. (1992). Some aspects of the Late- and Post-Variscan Development of the NW-German Basin. *Tectonophysics*, 207:65–95.

Brink, H.-J., Franke, D., Hoffmann, N., Horst, W., and Oncken, O. (1990). Structure and Evolution of the North German Basin - The European Geotraverse: Integrative Studies, Results from the 5th Earth Science Study Centre. *European Science Foundation, Strasbourg*, pages 195–212.

Chen, C.C. and Chen, C.S. (2000). Preliminary report on the Sanyi-Puli seismic zone conductivity anomaly and its correlation with velocity structure and seismicity in the Northwestern Taiwan. *Earth Planets Space*, 52:77–381.

DEKORP-BASIN Research Group (1999). The deep crustal structure of the Northeast German basin: new DEKORP-Basin'96 deep-profiling results. *Geology*, 27:55–58.

Duveneck, E. (2004). Velocity model estimation with data-derived wavefront attributes. *Geophysics*, 69:265–274.

Hengesbach, L. (2006). Magnetotellurische Studien im Nordwestdeutschen Becken: Ein Beitrag zur paläogeographischen Entwicklung des Unterkarbons. *PhD Thesis, Institut für Geophysik, Universität Münster*.

Hoecht, G. (2002). Traveltime approximations for 2D and 3D media and kinematic wavefield attributes. *PhD Thesis, Universität Karlsruhe*.

Hoffmann, N. and Brink, H.-J. (2001). Zur Struktur und Genese des tieferen Untergrundes des Norddeutschen Beckens - Ergebnisse der Interpretation langzeitregistrierter Steilwinkelseismik. *Mitteilungen Deutsche Geophysikalische Gesellschaft, DGG-Kolloquium "Interpretation reflexionsseismischer Messungen", Frankfurt*, pages 29–49.

Kockel, F. (2002). Rifting processes in NW-Germany and the German North Sea Sektor. *Geologie en Minjnbouw*, 81:149–158.

Mann, J. (2002). Extensions and applications of the Common-Reflection-Surface Stack Method. *Logos Verlag, Berlin*.

Maystrenko, Y., Bayer, U., and Scheck-Wenderoth, M. (2005). The Glueckstadt Graben, a sedimentary record between the North and Baltic Sea in north central Europe. *Tectonophysics, Special Issue*, 397:113–126.

Maystrenko, Y., Stovba, S., Stephenson, R., Bayer, U., Menyoli, E., Gajewski, D., Huebscher, C., Rabbel, W., Saintot, A., Starostenko, V., Thybo, H., and Tolkunov, A. (2003). Crustal-scale pop-up structure in cratonic lithosphere: DOBRE deep seismic reflection study of the Donbas fold belt, Ukraine. *Geology*, 31:733–736.

Menyoli, E., Gajewski, D., and Huebscher, C. (2004). Imaging of inverted basin structures with the CRS stack method. *Geophysical Journal International*, 157:1206–1216.

Müller, T. (1999). The Common Reflection Surface Stack Method. Seismic imaging without explicit knowledge of the velocity model. *PhD Thesis, University of Karlsruhe*.

Reichert, J.C. (1993). Ein geophysikalischer Beitrag zur Erkundung der Tiefenstruktur des Nordwestdeutschen Beckens längs des refraktionsseismischen Profils Norddeutschland 1975/76. *Geol. Jb.*, E50:3–87.

Scheck-Wenderoth, M. and Lamarche, J. (2005). Crustal memory and basin evolution in the Central European basin sysem - new insights from a 3D structural model. *Tectonophysics*, 397:143–165.

Schleicher, J., Tygel, M., and Hubral, P. (1993). Parabolic and hyperbolic paraxial two-point traveltimes in 3D media. *Geophysical Prospecting*, 41(4):495–514.

Snelson, C., Keller, G., Miller, K., Rumpel, H., Prodehl, C., and Levander, A. (2002). Crustal Growth in the Rocky Mountains Based on Seismic Refraction/Wide-Angle Reflection Data. *AGU Fall Meeting abstracts*.

Trappe, H. (1989). Deep seismic profiling in the North German Basin. *First Break*, 7:173–184.

Trappe, H., Gierse, G., and Pruessmann, J. (2001). The Common Reflection Surface (CRS) stack - structural resolution in Time Domain beyond the conventional NMO/DMO Stack. *First Break*, 19:625–633.

Tygel, M., Müller, T., Hubral, P., and Schleicher, J. (1997). Eigenwave based multiparameter traveltime expansions. *67th Annual Internat. Mtg., Soc. Expl. Geophys. Expanded Abstract*, pages 1770 – 1773.

Vieth, K.-U. (2001). Kinematic wavefield attributes in seismic imaging. *PhD Thesis, Fak. f. Physik, Universität Karlsruhe*.

Yegerova, T., Maystrenko, Y., Bayer, U., and Scheck-Wenderoth, M. (2006). The Glueckstadt Graben of the North-german Basin: new insights into the structure from 3D and 2D gravity analysis. *International Journal of Earth Sciences, submitted 2006*.

Zaske, J., Keydar, S., and Landa, E. (1999). Estimation of kinematic wave front parameters and their use for multiple attenuation. *Journal of Applied Geophysics*, 42(3-4):333–346.